

Tutorial: Tying a well to seismic using a blocked sonic log

Donald A. Herron¹

Abstract

Well ties to seismic data establish the fundamental link between geology as we measure it in a well bore and the seismic expression of geology that we work with as interpreters. This tutorial presents an example of tying a well to time-processed seismic data using a blocked sonic log for a case in which neither a vertical seismic profile, a synthetic seismogram, nor a check-shot survey is available. The described procedure requires only pencil and paper to quickly produce an acceptable well tie.

Introduction

Tying a well to seismic data is one of the most important tasks for a geoscientist in most if not all subsurface interpretation projects (see [Peterson et al. \[1955\]](#) for a historical perspective on the close relationship between seismic data and well logs). The tie is most accurately made when well-based reflectivity, in the form of either a vertical seismic profile (VSP) or a synthetic seismogram, is correlated to the seismic data. In this tutorial, I will deal only with time-processed data and will not address concerns and techniques for tying wells to depth-processed data. Unfortunately, there are cases in which a VSP was not acquired or a synthetic seismogram was or could not be generated, and a time-depth relationship is used to establish the tie from depth points on logs to their correlative reflection times on the seismic data. The major shortcoming in such an instance is that neither an actual seismic response (VSP) nor a modeled seismic response (synthetic seismogram) is used for correlation.

Most often, a well velocity or check-shot survey is the source of a direct time-depth relationship for tying a well to seismic, but again, there are cases in which such a survey wasn't acquired and the only source of velocity data, that is, time-depth data, is a sonic log. For this purpose, the sonic log is integrated, which involves summing transit times between adjacent depth samples in the log to create the needed time-depth relationship. This process can be approximated by a technique known as "blocking" the sonic log, which involves defining discrete intervals on the log over which a constant interval transit time (ITT), which corresponds to a constant *interval velocity*, is an acceptable approximation for the actual velocity character of the log. The series of blocked intervals and their associated ITTs are used to correlate the positions in time of the bound-

daries between the defined intervals on the log to their corresponding positions on the time-processed seismic data. The following section describes the details of this procedure applied to the Desoto Canyon 269 no. 1 well in the eastern Gulf of Mexico. Biostratigraphic data for this well were not available for this study, and so, formation tops corresponding to specific group and formation names are not assigned to individual reflections as part of the well tie.

Description of well and seismic data

The Desoto Canyon 269 no. 1 well on the "Shiloh" prospect was drilled as a straight hole by Shell and partners in 2003 to a total depth of 7318 m (24,009 ft) TVD as a discovery in Upper Jurassic Norphlet Aeolian sand. Figure 1 shows the chronostratigraphy of Jurassic and Lower Cretaceous strata in the eastern Gulf of Mexico as extrapolated from the eastern Gulf Coast (after [Mancini et al., 2008](#)), and Figure 2 shows the gamma ray, sonic, and density logs for the Desoto Canyon 269 no. 1 well.

The seismic line in Figure 3 is from a 3D survey in the eastern Gulf of Mexico jointly acquired and processed by PGS and TGS in 2008–2009. It is a Kirchhoff prestack time-migrated image displayed using the SEG polarity standard for a zero-phase reflection ([Sheriff, 2002](#)), in which, for a zero-phase wavelet, a positive reflection coefficient is represented by a central peak (plotted black as shown in Figure 4). Without having established the phase of these data via wavelet extraction, inspection of the seafloor reflection suggests that the data are close to zero phase (see Figure 5). Although visual estimation of the wavelet phase is not absolute or fool-proof, it is often the only means available to an interpreter when there is neither the time nor the means for quantitative wavelet extraction. A good rule of

¹Sugar Land, Texas, USA. E-mail: dherron7@gmail.com.

Manuscript received by the Editor 13 August 2013; revised manuscript received 7 October 2013; published online 20 March 2014; corrected version published online 10 April 2014. This paper appears in *Interpretation*, Vol. 2, No. 2 (May 2014); p. SD1–SD7, 10 FIGS., 2 TABLES.

<http://dx.doi.org/10.1190/INT-2013-0123.1>. © 2014 Society of Exploration Geophysicists and American Association of Petroleum Geologists. All rights reserved.

thumb is that an interpreter's eye can estimate the wavelet phase to $\pm 30^\circ$ given a reference boundary with known impedance contrast such as the seafloor, and in this example, the phase of the seafloor reflection is

probably between 0° and -30° . In the absence of any further analysis and as a reasonable approximation, in this example the procedure described in the following section assumes that the phase of the data is zero and does not change with reflection time.

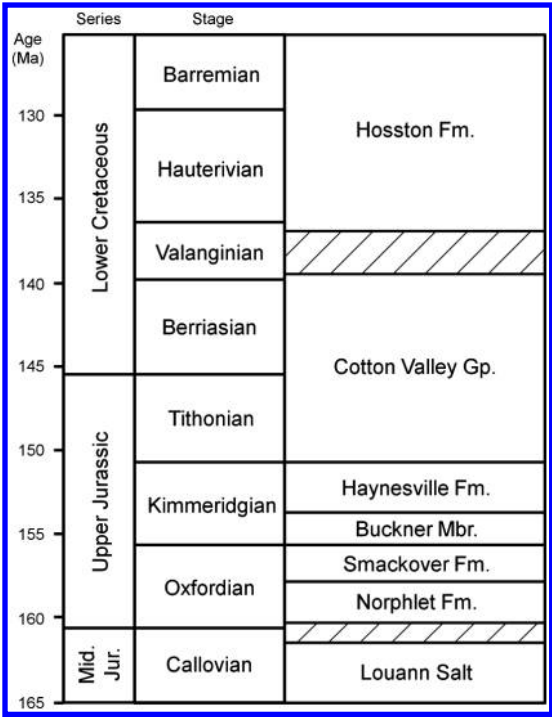


Figure 1. Chronostratigraphy of Jurassic and Lower Cretaceous strata in the eastern Gulf of Mexico as extrapolated from the eastern Gulf Coast (after Mancini et al., 2008).

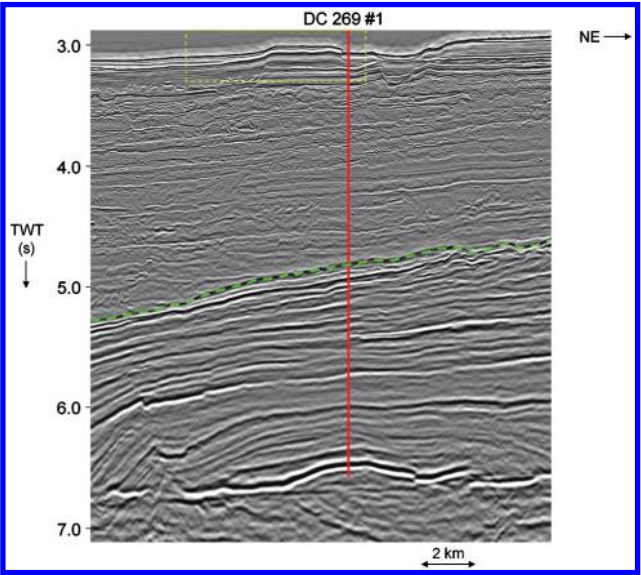
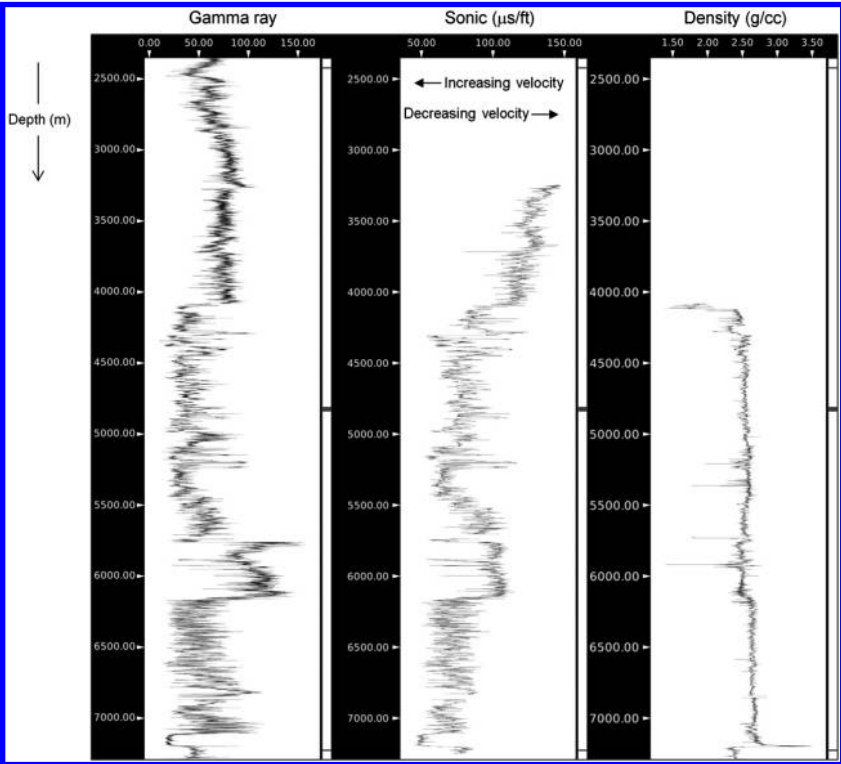


Figure 3. The 3D Kirchhoff prestack time-migrated line through the Desoto Canyon 269 no. 1 well. The dashed yellow box outlines the area enlarged in Figure 5. The dashed green horizon marks the approximate base of the Neogene clastic section based on regional seismic correlations.

Figure 2. Gamma ray, sonic, and density logs for the Desoto Canyon 269 no. 1 well. Depths are in meters below the drill floor.



Procedure

1) At the outset, ensure that the positioning of both the well and the seismic data is accurate so that the tie will be done at the correct point on the seismic data. This is usually straightforward for 3D seismic data but can be problematic for 2D data owing to imaging effects and projection into the seismic line.

2) Inspect the seismic data for prominent reflections (for example, sequence boundaries and unconformities) that have good continuity in the vicinity of the well and relatively strong amplitude above background reflectivity. For the data shown in Figure 6, five reflections annotated 1–5 with increasing reflection time were selected, reflection 1 corresponding to the base of the Neogene clastic section annotated on Figure 3. Note that reflections 1, 2, and 4 are peaks, 3 is a trough, and 5 is the peak in a symmetric peak-over-trough pair. The observation about reflection 5 suggests that it might be a tuned response.

3) Ensure that logs have been edited as necessary to remove spikes or other spurious features. Inspect the sonic and density logs for distinct step changes and departures from their general trends, and look for

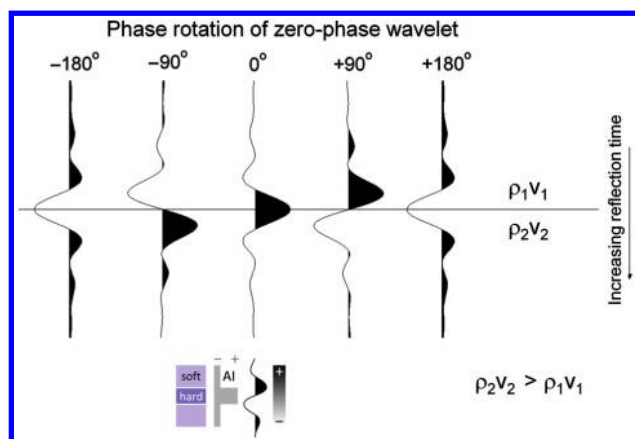


Figure 4. Illustration of a zero-phase wavelet, displayed in variable area wiggle trace format, rotated from -180° through $+180^\circ$ in increments of 90° (after Herron, 2011). The diagram at the bottom of the figure relates variable area wiggle and variable density trace display formats. A good rule of thumb is that an interpreter's eye can estimate the wavelet phase to $\pm 30^\circ$ given a reference boundary with a known impedance contrast such as the seafloor.

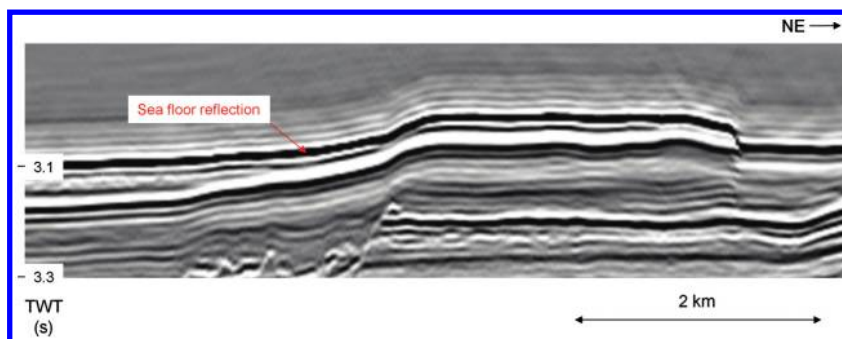


Figure 5. Enlargement of part of Figure 3 for visual inspection of the seafloor reflection. The character of this reflection suggests that the phase of the seismic data is probably between 0° and -30° .

intervals that can be reasonably and accurately approximated by constant values. Make note of the points at which both logs exhibit these changes, keeping in mind what the sign of the reflection coefficient would be at each point or boundary if you were to calculate an acoustic impedance log from the sonic and density logs (you are actually beginning to imagine what the synthetic seismogram might look like in doing this). Figure 7 shows the location of five boundaries annotated as markers α through ϵ across which there are distinct changes in the values measured by either the sonic or density log or both; the intervals defined by these boundaries are labeled A through D in the figure. Also annotated in Figure 7 is the sign of the impedance contrast expected at each boundary. Note that interval B probably could be divided into several smaller intervals, but as a first approximation, a single thick interval is used for blocking. Finer subdivision of interval B would most likely enable a more detailed tie to reflections corre-

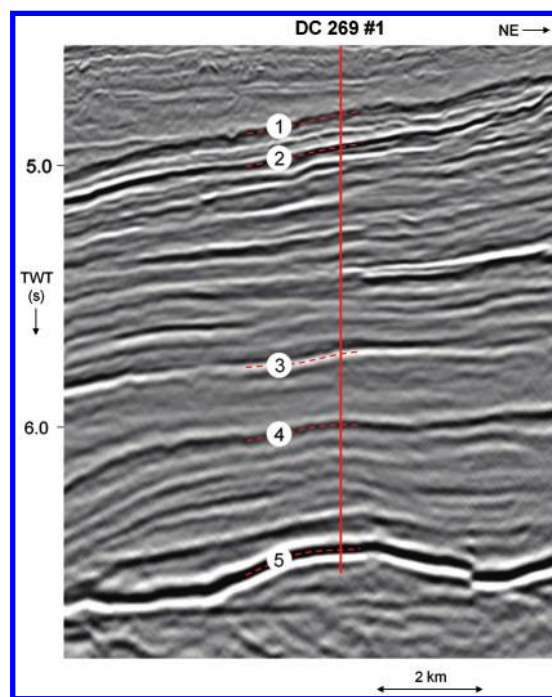


Figure 6. Enlargement of Figure 3 on which five reflections numbered 1–5 are annotated for correlation to the Desoto Canyon 269 no. 1 well.

sponding to the boundaries between these smaller intervals.

4) Block the sonic log according to the boundaries identified in step 3 to define intervals having constant ITTs. In simplest terms, blocking is the visual averaging of log values over specified intervals; in this example, the ITT for each blocked interval on the sonic log has an estimated uncertainty of $\pm 5 \mu\text{s}/\text{ft}$. Figure 8 shows the blocked sonic log for the Desoto Canyon 269 no. 1 well, and Table 1 lists the ITTs for each interval. Note that the section above marker α is characterized by a linear ITT gradient rather than a constant value.

5) For each blocked interval, calculate the two-way traveltime by dividing the interval thickness from the log by the constant ITT chosen for the blocked interval. Be sure to keep the units straight; a sonic log measures ITT in microseconds per unit length, but the seismic data to which the traveltime will be correlated are in milliseconds two-way traveltime (TWT). Hence, we have the following equation:

$$\text{two-way traveltime (ms)} = [2 * \text{ITT}(\mu\text{s}/\text{ft}) * \text{interval thickness from log (ft)}] / (1000 \mu\text{s}/\text{ms}). \quad (1)$$

6) Beginning with interval A, compare the two-way traveltime calculated for this interval in step (5) with the measured seismic TWT from reflection 1 to reflection 2. If desired, you can iterate this calculation with a slightly different value from the original blocked value but within a reasonable range for this value until achieving a close match with the measured seismic TWT for the interval between reflections 1 and 2 (see Table 1).

7) Continue these comparisons and iterative calculations for intervals B through D and reflections 2 through 5 to confirm which log marker corresponds to which reflection. Note that if there is not close correspondence between the seismic and log-based interval TWT values, then the interval boundaries on the blocked logs or the ITT values assigned to the blocked intervals, or both, need to be adjusted. The complete

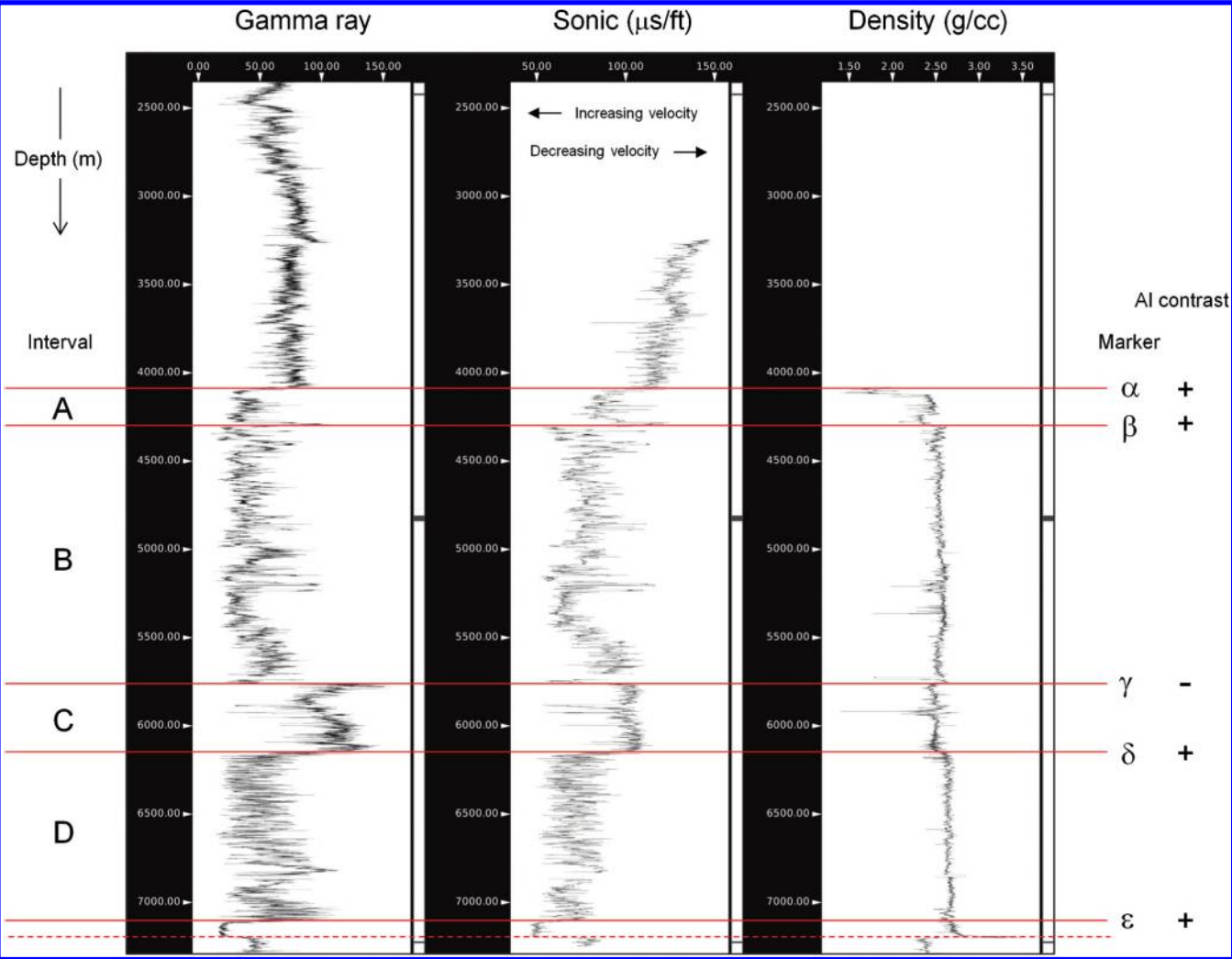


Figure 7. Same as Figure 2 showing log markers annotated α through ϵ , which define log intervals A through D. Each marker is at a boundary across which there is an abrupt change in the value of the sonic and/or density log.

Table 1 shows these calculations and enables comparison of the well- and seismic-based calculations and measurements of interval thickness. Note that the peak for reflection 5 and its following trough are in fact a tuned response to the high-velocity Smackover Limestone immediately overlying the Norphlet section (Her-ron, 2013).

A complete interval velocity-depth plot from the sea surface to reflection 5 can be constructed using the information from steps 5 through 7 together with interval velocities for seawater and the section above reflection 1. The interval velocity of seawater is calculated using the known water depth and the observed two-way reflection time to the seafloor reflection at the well

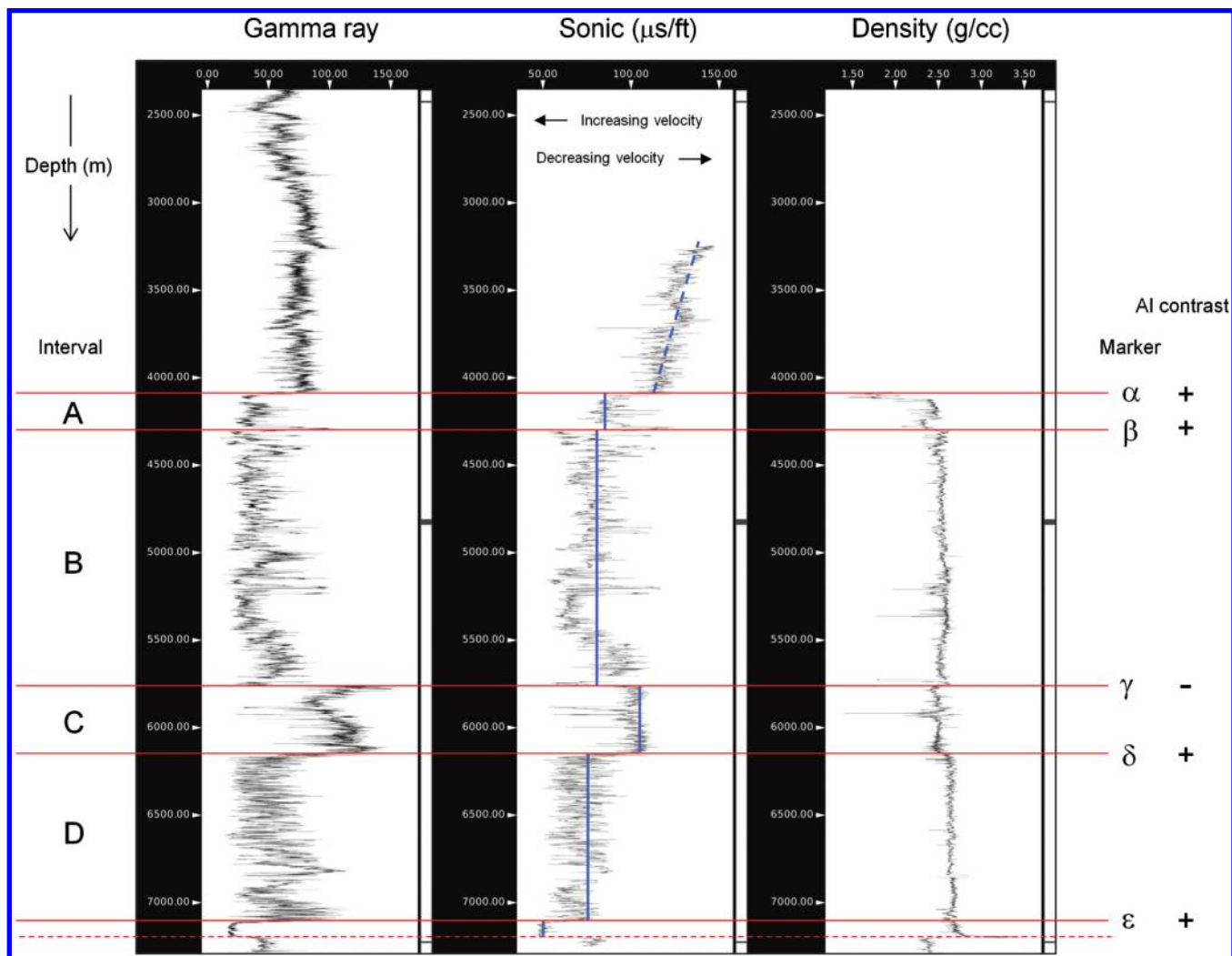


Figure 8. Same as Figure 7 with blocked values for the sonic log shown in blue. ITT values for the blocked sonic log are listed in Table 1.

Table 1. Depth and blocked sonic log data for the Desoto Canyon 269 no. 1 well.

Interval boundary	Depth subsea (ft)	Depth subsea (m)	Interval thickness (ft)	Interval thickness (m)	ITT ($\mu\text{s}/\text{ft}$)	Interval TWT (ms)	Iterate ITT to match seismic ($\mu\text{s}/\text{ft}$)
Top A	13,445	4098	685	209	85 ± 5	116	87.5
Top B	14,130	4307	4770	1454	80 ± 5	763	83.0
Top C	18,900	5761	1265	386	105 ± 5	266	107.5
Top D	20,165	6146	3160	963	75 ± 5	474	75.3
Base D	23,325	7109	—	—	—	—	—

location. Having tied the well at reflection 1, the interval velocity of the section from the seafloor to reflection 1 is calculated using the thickness in depth of this section and the observed two-way reflection time from the seafloor to reflection 1. The results of these calculations are shown in Table 2, and the resulting interval velocity-depth plot is shown in Figure 9.

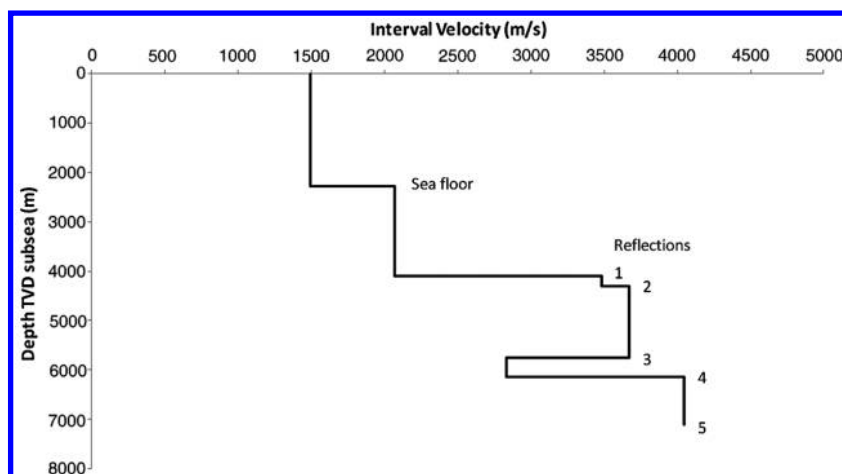
Figure 10 illustrates the final correlation of blocked log intervals A through D to reflections 1–5 on the seismic line having graphically stretched the sonic log interval by interval from depth to time. In the author's opinion, this is an acceptable well-to-seismic tie, given the available data and using the procedure described in this tutorial, for the following reasons (as mentioned previously, the lack of biostratigraphic data for the Desoto Canyon 269 no. 1 well precludes assignment of formation tops to individual reflections as part of the well tie):

- 1) The blocking of the sonic log is reasonable in view of the overall log character.

Table 2. Time, depth, and interval velocity data for the Desoto Canyon 269 no. 1 well to seismic tie.

Marker	Observed seismic TWT (ms)	Observed seismic TWT (ms)	Depth subsea (ft)	Depth subsea (m)	Interval velocity (ft/s)	Interval velocity (m/s)
Sea level	0	—	0	0	—	—
Seafloor	3062	3062	7509	2289	4905	1495
1	4810	1748	13,445	4098	6792	2070
2	4930	120	14,130	4307	11,417	3480
3	5722	792	18,900	5761	12,045	3671
4	5994	272	20,165	6146	9301	2835
5	6470	476	23,325	7109	13,277	4047

Figure 9. Interval velocity-depth plot for the Desoto Canyon 269 no. 1 well. The time, depth, and velocity data used to construct this plot are shown in Table 2.



- 2) Based on personal experience, the interval velocities calculated from the ITT values on the blocked sonic log are well within the range of interval velocities for Mesozoic rocks in the Desoto Canyon area and elsewhere in the eastern Gulf of Mexico.
- 3) The log markers converted to time using the interval velocities derived from the blocked sonic log correlate well with the prominent reflections on the seismic data, and the sign of the impedance contrast for

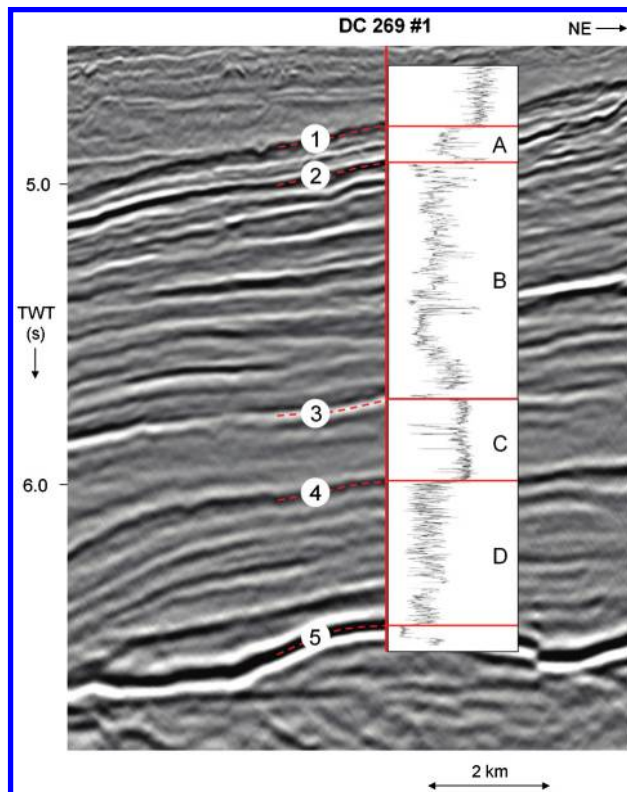


Figure 10. Final correlation of blocked log intervals A through D on the Desoto Canyon 269 no. 1 well to reflections 1–5 on the 3D PSTM line shown in Figure 6.

each marker matches the polarity of its correlative reflection.

- 4) The log markers can be confidently correlated to the seismic data without need for excessive adjustment of the blocked log values.

Conclusions

The nature of seismic interpretation is such that we often have to work with fewer data than we would prefer to have. With more data, we might be able to reach conclusions with greater confidence, but we don't always enjoy the luxury or good fortune of having those data. This tutorial illustrates a technique based on fundamental principles that you can use to make a good well tie in less-than-ideal circumstances. You should note that other than using machine-generated log and seismic displays, the entire procedure described in this tutorial can be done with pencil and paper in a reasonably short time.

Acknowledgments

The author thanks R. Newrick, P. Anderson, C. Cabarcas, and B. Babangida for their very helpful comments and suggestions and also PGS and TGS for permission to show their data.

References

- Herron, D. A., 2011: First steps in seismic interpretation: SEG, Geophysical Monograph Series, no. 16.
- Herron, D. A., 2013, Thoughts and observations on interpreting depth-imaged data: *Interpretation*, **1**, no. 1, B1–B6, doi: [10.1190/INT-2012-0020.1](https://doi.org/10.1190/INT-2012-0020.1).

Mancini, E. A., J. Obid, M. Badali, K. Liu, and W. C. Parcell, 2008, Sequence-stratigraphic analysis of Jurassic and Cretaceous strata and petroleum exploration in the central and eastern Gulf coastal plain, United States: AAPG Bulletin, **92**, 1655–1686, doi: [10.1306/08130808046](https://doi.org/10.1306/08130808046).

Peterson, R. A., W. R. Fillippone, and F. B. Coker, 1955, The synthesis of seismograms from well log data: *Geophysics*, **20**, 516–538, doi: [10.1190/1.1438155](https://doi.org/10.1190/1.1438155).

Sheriff, R. E., 2002, Encyclopedic dictionary of applied geophysics, 4th ed.: SEG, Geophysical References Series, no. 13.



Don Herron received a B.S. with honors (1971) in geological sciences from Brown University and an M.S. (1973) in geological sciences from the California Institute of Technology. He enjoyed a career as a seismic interpreter at Texaco (1973–1977), Gulf (1977–1984), and most recently Sohio/BP (1984–2008). Since retirement in 2008, he has worked as an independent geophysical consultant for Petroleum Geo-Services (PGS) as a geosciences advisor and with several oil companies as a seismic interpretation instructor. At Gulf and Sohio/BP, he taught in-house courses in seismic interpretation and was coinstructor for the SEG continuing education course “Seismic Interpretation in the Exploration Domain” (1995–2007). He was a member of the editorial board of *The Leading Edge* (2002–2007, chairman in 2006–2007) and is the author of the bimonthly “Interpreter Sam” column in *The Leading Edge*. He is an active member of SEG, AAPG, and Sigma Xi.

This article has been cited by:

1. Aminu A. Isyaku, Derek Rust, Richard Teeuw, Malcolm Whitworth. 2016. Integrated well log and 2-D seismic data interpretation to image the subsurface stratigraphy and structure in north-eastern Bornu (Chad) basin. *Journal of African Earth Sciences* **121**, 1-15. [[CrossRef](#)]
2. Mattia Aleardi. 2015. Seismic velocity estimation from well log data with genetic algorithms in comparison to neural networks and multilinear approaches. *Journal of Applied Geophysics* **117**, 13-22. [[CrossRef](#)]